

The Second Cambridge Pulsar Survey at 81.5 MHz

J. A. Shrauner¹, J. H. Taylor²

Joseph Henry Laboratories and Physics Department
Princeton University, Princeton, NJ 08544

G. Woan³

Mullard Radio Astronomy Observatory, Cavendish Laboratory
Cambridge University, Cambridge CB3 OHE, UK

ABSTRACT

We have searched the northern sky for pulsars at the low radio frequency of 81.5 MHz, using the 3.6-hectare array at Cambridge, England. The survey covered most of the sky north of declination -20° and provided sensitivities of order 200 mJy for pulsars not too close to the galactic plane. A total of 20 pulsars were detected, all of them previously known. The effective post-detection sampling rate was 1.3 kHz, and the sensitivity to low-dispersion millisecond pulsars was sufficient to allow the detection of objects similar to PSR J0437-4715 (period 5.7 ms, dispersion measure $2.6 \text{ cm}^{-3}\text{pc}$, mean flux density $\sim 1 \text{ Jy}$). No such pulsars were found.

Subject headings: pulsars — surveys

1. Introduction

Pulsars were discovered in 1967 when Bell and Hewish were observing the interplanetary scintillations (IPS) of compact radio sources, using a fixed dipole array at 81.5 MHz (Hewish *et al.* 1968). Chart recordings were examined by eye for evidence of intrinsically pulsed signals, which looked somewhat different from the scintillating quasars being studied. Within

¹Present address: WebTV Network, 1295 Charleston Road, Building B, Mountain View, CA 94043; shrauner@corp.webtv.net

²joe@pulsar.princeton.edu

³Present address: Department of Physics & Astronomy, University of Glasgow, Glasgow G12 8QQ, UK; graham@astro.gla.ac.uk

a few months, the first Cambridge pulsar search discovered a total of six pulsars: PSRs B0329+54, B0809+74, B0834+06, B0950+08, B1133+16, and B1919+21 (Hewish *et al.* 1968, Pilkington *et al.* 1968, Cole & Pilkington 1968). Soon afterward the dipole array returned to nearly full-time studies of IPS, compact radio sources, and the interplanetary medium—the purposes for which it had been designed.

Most pulsar searching since 1968 has been done at radio frequencies around 400 MHz and higher, where the sky background is lower, interstellar dispersion and scattering are less of an impediment, and much larger bandwidths can be gainfully used. Nevertheless, in 1993 it seemed to us for a number of reasons that a second Cambridge pulsar search at 81.5 MHz would be a worthwhile undertaking. The IPS dipole array has been doubled in size since 1968, and now has a geometric collecting area of 36,055 m² or 3.6 hectares—approximately half that of the 305 m telescope in Arecibo, Puerto Rico. The discovery of PSR J0437–4715 by Johnston *et al.* (1993) demonstrated the existence of at least one very strong, nearby, millisecond pulsar. We reasoned that if similar pulsars exist in the northern sky, the 3.6-hectare array should be capable of detecting them, especially if their low-frequency radio spectra are steeper than those of most slowly rotating pulsars, as suggested by Foster *et al.* (1991). Fortunately, the nature of the Cambridge array is such that co-opting any one of its 16 simultaneous beams for pulsar searching can be done with only minimal disruption to its continuing IPS studies.

2. The Telescope

The 3.6 hectare array is a meridian-transit instrument consisting of 4096 full-wave dipoles operating at a wavelength $\lambda = 3.68$ m. The dipoles are arranged in 32 east-west rows of 128 dipoles each, with a spacing between rows of $d = 0.65$ wavelengths. A branched feeder network combines the signals within each row, properly phasing them for a celestial source on the meridian. Summed signals from the 16 northern-most and 16 southern-most rows are then combined in a matched pair of “Butler matrices” to form simultaneous beams at 16 declinations in the range $-8^\circ < \delta < 90^\circ$. For IPS studies the two half-arrays are used as a north-south phase-switching interferometer (Purvis *et al.* 1987); however, for our pulsar observations we connected the two halves as a total-power phased array. A modified set of 16 beams can be generated by inserting an extra phase gradient in the north-south direction across the entire array, thereby shifting each beam north by half a beamwidth, or about 3° .

The declination of the peak response for each of the 32 possible beams is given by

$$\delta_0(N) = 52.16^\circ + \arcsin \left[\frac{\lambda(N-10)}{16d} \right], \quad (1)$$

where the beam number, N , is an integer in the range 1–16 for the unshifted beams, and a half-integral value between 1.5 and 16.5 for the shifted beams (Purvis 1981, Purvis *et al.* 1987). The beams have half-power widths of $5.5^\circ / \cos [52.16^\circ - \delta_0(N)]$ in declination. A reflecting screen lies $\lambda/4$ beneath each row, and is inclined towards the south at 50 degrees to the vertical in order to increase the sensitivity of the array at lower declinations. However, Tappin (1984) has shown that the declination power response, D , of the antenna follows that expected for an array of dipoles $\lambda/4$ above a flat, horizontal reflecting screen; he finds no evidence for increased sensitivity at lower declinations.

Let η represent the angle of the reflecting screen to the horizontal, and define the following three additional angles:

$$\phi \equiv 52.16^\circ - \delta, \quad (2)$$

$$\psi \equiv \left(\frac{\pi d}{\lambda} \right) \sin \phi + \left(\frac{N - 10}{16} \right) \pi, \quad (3)$$

$$\alpha \equiv \left(\frac{32\pi d}{\lambda} \right) \sin \phi. \quad (4)$$

The normalized declination power response can then be expressed as

$$D(N, \delta) = \left(\frac{1 \pm \cos \alpha}{2} \right) \sin^2 \left[\frac{\pi}{2} \cos(\phi - \eta) \right] \frac{\sin^2 16\psi}{16^2 \sin^2 \psi}, \quad (5)$$

where the three factors on the right-hand side arise from the interference between the two array halves, the reflecting screen, and the 16 phased rows in each half, respectively. Following Tappin, we take $\eta = 0$. Inserting the peak-response declinations of equation (1) into equation (5) then shows that D is maximized by phasing the array so as to use the plus sign in the first factor for integral beam numbers, and the minus sign for half-integral beam numbers. The top panel of Figure 1 shows the combined declination response afforded by the antenna for the whole survey, obtained by summing the calculated power responses of all 32 beams.

The peak gain of each beam is proportional to the effective collecting area of the array, which falls off as the cosine of zenith angle. Because of this foreshortening, several of the beams have secondary responses comparable to or even greater than their primary responses. As examples, the bottom panel of Figure 1 shows the individual power responses of beams 1 (solid curve) and 10 (dashed curve). The true declinations of sources detected in the beams with large secondary responses can be determined from their transit times through the east-west beam: a source at declination δ has a half-power transit time of $107/\cos \delta$ seconds (Purvis 1981). For the secondary responses at $\delta > 90^\circ$, transit times are shifted by 12 hours.

3. Observations and Data Analysis

Our observations were carried out between November 1993 and June 1994. We phased the array for a given beam number, $N = 1, 1.5, 2, 2.5, \dots, 16.5$, and recorded data continuously for 24 hours as the sky drifted overhead. Observations were repeated as demanded by interference, equipment malfunction or mis-adjustment, etc., until each of the 32 beams had been observed and produced high-quality data at least twice. Figure 2 illustrates the full sky coverage of the survey. We analyzed beams 16 and 16.5 for signals entering via their secondary responses, rather than the primary ones. Consequently the survey provided useful sensitivity between declinations of -20° and $+86^\circ$, with a few small areas missing because of interference. Note, however, that because of array foreshortening at low declinations and the “scalloped” overall response as a function of δ , as well as the large variation in background temperature over the sky, our sensitivity even to low-dispersion, long period pulsars varied by more than an order of magnitude over the surveyed area. As described in more detail below, the median sensitivity for low-dispersion pulsars with periods $P > 0.1$ s was about 200 mJy.

When the 3.6-hectare array is being used solely for IPS observations, the southernmost 14 beams are observed simultaneously. We diverted a single beam on a given day for pulsar observations, thereby causing only minimal disruption to the IPS work. Signals from the two halves of the array, properly phased for the desired beam, were extracted from the two Butler matrices and added. The resulting signal was mixed to intermediate frequency of 10.7 MHz and then to baseband, using quadrature local oscillators. An automatic gain control served to keep the post-detection noise level constant. The in-phase (“real”) and quadrature (“imaginary”) baseband signals were low-pass filtered at 0.47 MHz (the filters are 60 dB down at 0.5 MHz), sampled at a 1 MHz rate, and digitized in a 12-bit analog-to-digital converter controlled by a programmable digital signal processor (DSP; Analog Devices ADSP-21020) on a VME board made by the Ixthos Corporation.

The incoming data were double-buffered in fast memory on the DSP board. At intervals of $256\ \mu\text{s}$ the ADSP-21020 performed a 256-point complex Fourier transform on the incoming data and squared the resulting magnitudes. Three consecutive power spectra were summed, and every $768\ \mu\text{s}$ the difference between the 256-channel power spectrum and an exponentially-weighted mean of spectra over the past 1.5 s was one-bit sampled. The resulting bits were packed into 32-bit words and passed to a controlling workstation, which wrote them onto magnetic tape along with the running averages and root-mean-square deviations of the summed power spectra and the date, time, and beam number. A full day’s observing session generated about 3.5 GB of data, which fit comfortably on a single 8 mm tape cassette.

Searching for pulsar signals was accomplished by reading the recorded data from tape

into another workstation. The one-bit data were unpacked and divided into consecutive blocks with length comparable to the beam transit time at the relevant declination. Block lengths of 2^{17} samples were used for beams 1–10, 16, and 16.5; 2^{18} samples for beams 10.5–13; and 2^{19} samples for beams 13.5–15.5. These numbers correspond to transit times of 101, 201, and 403 s. Beams 16 and 16.5 were processed using the short block length so as to remain sensitive to pulsars in their secondary responses at declinations near -20° and -13° , respectively. The total amount of computing was substantial: with the DEC AXP 3000/400 workstation used to do most of it, about 3.6 days of computing was required for each day of observations—nearly eight months of continuous computing, in all.

The search program analyzed each beam area independently. Progressive delays were introduced between the 256 spectral channels in a manner that optimally produces time series at different dispersion measures (Taylor 1974). Curvature in the delay-versus-frequency relation was compensated by shifting the middle two-thirds of the spectral channels by one channel. For each data block, the one-bit samples were optimally de-dispersed at 256 dispersion measures evenly spaced between 0 and $12.78 \text{ cm}^{-3}\text{pc}$. Additional dispersion ranges were generated by first adding successive pairs of time samples in each spectral channel, and then reapplying the de-dispersion algorithm. The de-dispersed time series in each new range thus had half the length of those in the previous range, and the upper half of each group of dispersions extended the ranges of those already computed. In this manner, each data block was also de-dispersed by 128 dispersion measures evenly spaced across each of the following ranges: 12.83–25.60, 25.65–51.25, and 51.30–102.55 cm^{-3}pc .

For each data block a total of 640 de-dispersed time series were Fourier transformed and analyzed for harmonic content. After removing known sources of periodic interference (in particular, the 274 Hz phase-switching frequency used for IPS studies), the search program identified the strongest periodicities by interpolating between the complex Fourier coefficients and finding the peak amplitudes, and also by summing harmonically related frequencies in groups of 2, 3, 4, 8, and 16 harmonics. The program isolated the most promising pulsar suspects in the frequency domain, formed the equivalent integrated pulse shapes by transforming complex coefficients (with up to 32 harmonics) back into the time domain, and computed their signal-to-noise ratios. Any suspect detections with signal strengths above a predetermined threshold were presented as possible detections.

4. Flux Density Measurements and Survey Sensitivity

The expected signal-to-noise ratio, \mathcal{R} , of a received pulsar signal can be related to various system parameters by the expression

$$\mathcal{R} = \frac{\eta_Q S_{81} G}{T_{\text{sys}}} \left[\frac{(B\tau n_p)(P-w)}{w} \right]^{1/2}, \quad (6)$$

where η_Q is the digitization efficiency factor, S_{81} the mean flux density of the pulsar at 81.5 MHz (Jy), G the telescope gain (K Jy⁻¹), T_{sys} the system temperature (K), B the bandwidth (Hz), τ the integration time (s), n_p the number of polarizations, P the period, and w the pulse width. Our system had $B = 1$ MHz, $n_p = 1$, and because of the one-bit post-detection digitization, $\eta_Q = \sqrt{2/\pi}$ (Dewey *et al.* 1985, Thompson, Moran, & Swenson 1986). Flux density measurements can therefore be obtained for detected pulsars by determining G/T_{sys} from calibration measurements, calculating \mathcal{R} , P , and w from average profiles, and solving for S_{81} .

The appropriate value of G for any direction in our surveyed region depends on variations in antenna gain across the declination strip, the peak gain and sidelobe responses of the different beams, and the background sky temperature. The first effect can be calculated from the declination power response given by equation (5), and the latter two by using a sky map of equivalent background flux density obtained with the same telescope. Figure 4.5.2 of Purvis (1981) presents a contour map of the system noise level of the 3.6-hectare array when operated as a phase-switching interferometer. The contour levels indicate twice the receiver noise level, in Janskys, for a bandwidth $B = 1$ MHz and integration time $\tau_{\text{map}} = 0.33$ s. The map therefore plots the flux density S_{map} at which unresolved, continuous sources at the beam centers would be detected with signal-to-noise ratio $\mathcal{R} = 2$. At an arbitrary declination δ close to the strip-center at δ_0 , we have

$$\frac{G}{T_{\text{sys}}} = \frac{2(B\tau_{\text{map}})^{1/2}}{S_{\text{map}}} \frac{D(N, \delta)}{D[N, \delta_0(N)]}. \quad (7)$$

It therefore follows that the flux density of a pulsar observed with signal-to-noise ratio \mathcal{R} is given by

$$S = \mathcal{R} S_{\text{map}} \frac{D[N, \delta_0(N)]}{D(N, \delta)} \left[\frac{0.13w}{\tau(P-w)} \right]^{1/2}. \quad (8)$$

More than 10^8 possible combinations of period, dispersion measure, and pulse width are tested for significance in each data block, and consequently a moderately high threshold signal-to-noise ratio must be used to keep the rate of false detections low. We adopted a lower limit of $\mathcal{R} = 8.5$, and the sensitivity of the whole survey can therefore be characterized by

inserting this number into equation (8) together with appropriate values for the integration time, τ , and effective pulse width, w , including all forms of instrumental smoothing. The pulse width is bounded on the low side by Δt , the post-detection sample interval; it also depends on the dispersion measure. For periods smaller than $64\Delta t \approx 49.2$ ms in the lowest dispersion range, the minimum detectable flux density scales approximately as $P^{-1/2}$. Similar behavior obtains for the higher dispersion ranges, with the effective Δt doubling in each successive range. A more complete sensitivity analysis based on the detailed implementation of our search algorithm leads to the stepwise continuous sensitivity curves plotted in Figure 3 (see Nice, Fruchter, & Taylor 1995). This graph shows the sensitivity of our survey to a low-duty-cycle ($w \ll P$) pulsar in a region with the median sky background noise, $S_{\text{map}} = 2$ Jy. The curves show the minimum flux densities that yield $\mathcal{R} = 8.5$, as a function of period, and are plotted for five values of DM up to the largest values searched. Steps in the sensitivity curves occur at periods equal to multiples of Δt , where the number of harmonics tested by the search software changes. The sky background noise S_{map} varies between the extremes of 0.5 and 9 Jy, but is < 2 Jy for 50% and < 3 Jy for about 70% of the visible sky (Purvis 1981). It is important to note that the sensitivity models of equation (8) and Figure 3 do not explicitly account for interstellar scattering effects, which will likely dominate the pulse broadening for pulsars with $\text{DM} \gtrsim 50 \text{ cm}^{-3}\text{pc}$. Such pulsars always lie close to the galactic plane, and for this and other reasons are more profitably observed at frequencies much higher than 81.5 MHz.

5. Results

We detected a total of 20 pulsars, all of them previously known. Their locations are plotted in galactic coordinates in Figure 2. Table 1 lists their catalogued parameters including names, B1950 celestial coordinates, periods, dispersion measures, and 400 MHz flux densities, S_{400} . We also list the offsets, $\Delta\delta$, between each pulsar's location and the nearest beam center, as well as the observed signal-to-noise ratios for the two times each pulsar was nominally observed, and the average flux densities, S_{81} , for the positive detections. The signal-to-noise ratios are those determined by the search program for the closest beam pointing. We include values for both observations of the relevant declination strip to give some indication of the efficiency of the search algorithm and the repeatability of the measurements. Flux densities were calculated by applying equation (8) to the average profiles created by synchronously averaging one full beam-transit of data, centered on the pulsar's right ascension. The profile obtained in this way for each pulsar is illustrated in Figure 4.

The accuracy of our flux density measurements depends on calibration errors and manual

“readout uncertainties” of the sky map, as well as the degree to which the pulsar signals were affected by time-variable scintillation effects. The sky map is thought to be accurate to within about 20%, and the map-reading uncertainties probably contribute another 20% uncertainty. Interstellar scintillation causes significant modulations of the signal strengths by factors of 2 or more, particularly for the lowest-dispersion pulsars. Some information on internal consistency of the results may be gained from the 13 pulsars detected in each of the two days their declination strip was observed. Their flux density measurements show a root-mean-square deviation of 25% around the mean. Altogether we estimate that the flux density measurements are accurate to approximately 40%, and within such limits are in good accord with previous work. An especially low measured flux for PSR B0809+74 may be the result of uncertain extrapolation of sky-background contours near the edge of the map.

Radio-frequency spectra of the 20 detected pulsars are presented in Figure 5. Pulsar spectra are generally characterized by power-law indices of -1.5 to -2 at frequencies above a few hundred MHz; typically the spectra flatten and perhaps even turn over at lower frequencies. Low-frequency turnovers are clearly evident for some of the spectra displayed in Figure 5, and it seems certain that similar behavior in many other known pulsars prevented their detection in our survey. Even among the pulsars we detected, nearly half are an order of magnitude weaker at 81.5 MHz than would be expected from straight-line extrapolations of their higher-frequency spectra.

Not surprisingly, all six of the original Cambridge pulsars were detected in the survey, although PSR B0950+08 was one of the seven pulsars only seen in a single day’s observations. None of the seven pulsars seen only once would have been confirmed as a new pulsar discovery solely on the basis of the observations we made; however, further attempts at confirmation would have been undertaken for any candidate with a single observation as promising as these. PSR B0950+08 was actually observed during initial trial runs using only half the array, and also in some observations when the array was mistakenly anti-phased. Figure 5 shows variations more than an order of magnitude in measured fluxes of PSR B0950+08 around 100 MHz, with our measurement close to the top of the range. A scintillation-induced order-of-magnitude decrease in received flux would have rendered the pulsar undetectable in the survey. The strongest pulsar detected in our survey, PSR B2217+47, was not detected in the first Cambridge pulsar search because, with a $DM = 44 \text{ cm}^{-3}\text{pc}$, its pulse is smeared out over more than a full period in a 1 MHz bandwidth. Its pulses, and also those of PSRs B0919+06 and B1642–03, are quite undetectable with the Cambridge telescope, without the benefit of dispersion-removal techniques.

In the coldest regions of the sky the minimum detectable flux density of our survey is about 100 mJy. Several pulsars we did not see have been detected by others at frequen-

cies between 70 and 100 MHz, with mean flux densities greater than that minimum: PSRs B0138+59, B0320+39, B0523+11, B0525+21, B0531+21, B0611+22, B1612+07, B1842+14, B2111+46, B2154+40, and B2319+60 (Izvekova *et al.* 1981, Sieber 1973, Malofeev *et al.* 1994). Of these, PSR B2111+46 has a DM of $141.5 \text{ cm}^{-3}\text{pc}$, which exceeds the highest value we searched; and the pulsar in the Crab nebula, PSR B0531+21, is undetectable as a periodic source because interstellar scattering broadens its pulse excessively at 81.5 MHz. The remaining pulsars all have reported flux measurements below the detection threshold for their sky positions, periods, and dispersion measures, except for PSRs B0138+59 and B0320+39. Our estimated sensitivities at these positions are 150 and 420 mJy, respectively. Izvekova *et al.* (1981) report a flux measurement for PSR B0138+59 of 260 mJy at 85 MHz. Malofeev *et al.* (1994) quote fluxes for PSR B0320+39 of 700 and 500 mJy at 60 and 100 MHz, respectively, while Izvekova *et al.* (1981) give mean flux density measurements of 230 and 160 mJy at the same frequencies. It follows that these two pulsars would have been marginal detections in our survey, at best.

In summary, the second Cambridge pulsar survey detected all previously known pulsars in the northern hemisphere that we could have expected to detect, with the possible exception of PSR B0138+59. We obtained the lowest frequency flux measurements available for PSRs B0450+55, B0655+64, B1839+56, B2110+27, and B2224+65. Interestingly, PSR B0655+64 is a binary pulsar, with orbital period just slightly longer than a day. If it had been just a little stronger, and therefore had been discovered by Bell and Hewish in 1968, disentangling its orbiting nature by means of observations with this transit telescope would have been quite difficult — as indeed it still was, when the pulsar was discovered with the 300 ft transit telescope in Green Bank, a decade later (see Damashek *et al.* 1982). With respect to possible detections of millisecond pulsars, we offer the following comments. Over the northern celestial hemisphere our median sensitivity to pulsars similar to J0437–4715 ($P = 5.7 \text{ ms}$, $\text{DM} = 2.6 \text{ cm}^{-3}\text{pc}$, $S_{81} \approx 1 \text{ Jy}$; see McConnell *et al.* 1996) was approximately 0.7 Jy. If pulsars like PSR J0437–4715 were scattered all over the northern hemisphere, we would have detected more than half of them. We conclude, therefore, that such objects are quite rare. Almost certainly there is no such pulsar in our surveyed region with $S_{81} > 3 \text{ Jy}$.

We thank A. Hewish and R. Hills for organizational assistance in the early phases of this project, and J. Milrod and the Ixthos Corporation for their generous loan of the DSP hardware. Pulsar studies at Princeton are supported by the US National Science Foundation. G. W. thanks SERC (now PPARC) for a Research Fellowship and Clare College Cambridge for a College Lectureship, both held during the bulk of this work.

REFERENCES

Cole, T. W. & Pilkington, J. D. H. 1968, *Nature*, 219, 574

Damashek, M., Backus, P. R., Taylor, J. H., & Burkhardt, R. K. 1982, *ApJ*, 253, L57

Deshpande, A. A. & Radhakrishnan, V. 1992, *J. Astrophys. Astr.*, 13, 151

Dewey, R. J., Taylor, J. H., Weisberg, J. M., & Stokes, G. H. 1985, *ApJ*, 294, L25

Foster, R. S., Fairhead, L., & Backer, D. C. 1991, *ApJ*, 378, 687

Gupta, Y., Rickett, B. J., & Coles, W. A. 1993, *ApJ*, 403, 183

Hewish, A., Bell, S. J., Pilkington, J. D. H., Scott, P. F., & Collins, R. A. 1968, *Nature*, 217, 709

Izvekova, V. A., Kuz'min, A. D., Malofeev, V. M., & Shitov, Y. P. 1981, *Ap&SS*, 78, 45

Johnston, S. *et al.* 1993, *Nature*, 361, 613

Kuzmin, A. D., Malofeev, V. M., Shitov, Y. P., Davies, J. G., Lyne, A. G., & Rowson, B. 1978, *MNRAS*, 185, 441

Lorimer, D. R., Yates, J. A., Lyne, A. G., & Gould, D. M. 1995, *MNRAS*, 273, 411

Lyne, A. G. & Rickett, B. J. 1968, *Nature*, 219, 1339

Malofeev, V. M., Gil, J. A., Jessner, A., Malov, I. F., Seiradakis, J. H., Sieber, W., & Wielebinski, R. 1994, *A&A*, 285, 201

McConnell, D., Ables, J. G., Bailes, M., & Erickson, W. C. 1996, *MNRAS*, 280, 331

McLean, A. I. O. 1973, *MNRAS*, 165, 133

Nice, D. J., Fruchter, A. S., & Taylor, J. H. 1995, *ApJ*, 449, 156

Pilkington, J. D. H., Hewish, A., Bell, S. J., & Cole, T. W. 1968, *Nature*, 218, 126

Purvis, A. 1981. PhD thesis, Cambridge University

Purvis, A., Tappin, S. J., Rees, W. G., Hewish, A., & Duffett-Smith, P. J. 1987, *MNRAS*, 229, 589

Sieber, W. 1973, *A&A*, 28, 237

Sieber, W. & Wielebinski, R. 1987, A&A, 177, 342

Slee, O. B. & Hill, E. R. 1971, Aust. J. Phys., 24, 441

Stinebring, D. R. & Condon, J. J. 1990, ApJ, 352, 207

Tappin, S. J. 1984. PhD thesis, Cambridge University

Taylor, J. H. 1974, A&AS, 15, 367

Taylor, J. H., Manchester, R. N., & Lyne, A. G. 1993, ApJS, 88, 529

Taylor, J. H., Manchester, R. N., Lyne, A. G., & Camilo, F. 1995, Unpublished (available at <ftp://pulsar.princeton.edu/pub/catalog>)

Thompson, A. R., Moran, J. M., & Swenson, G. W. 1986, Interferometry and Synthesis in Radio Astronomy, (New York: John Wiley and Sons)

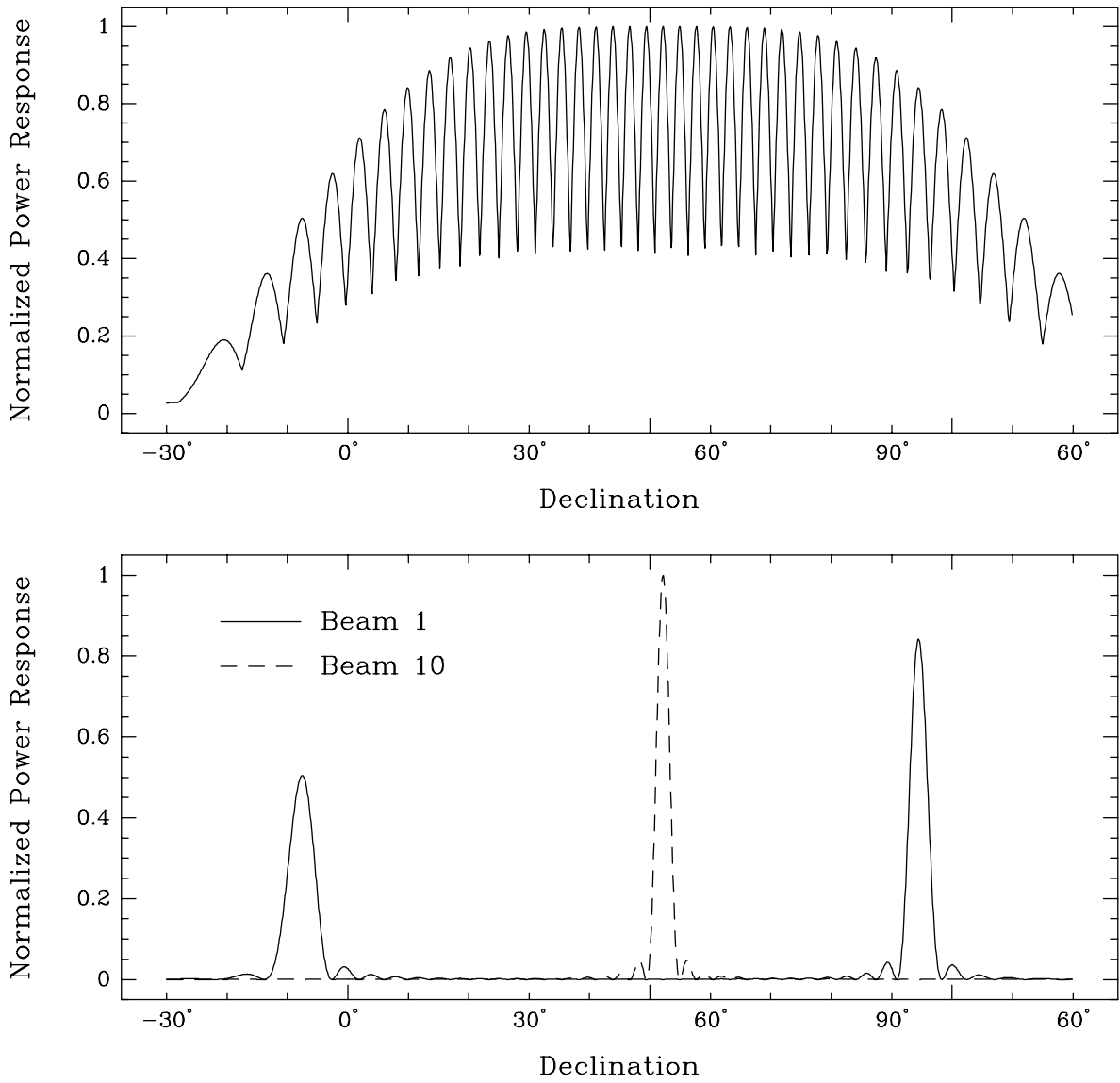


Fig. 1.— Normalized declination response of the 3.6-hectare array. *Top*: combined power response provided by all 32 beams. *Bottom*: full response patterns of beams 1 and 10. Note that beam 1 has a secondary response at $+94^\circ$ which is stronger than its primary response at -8° .

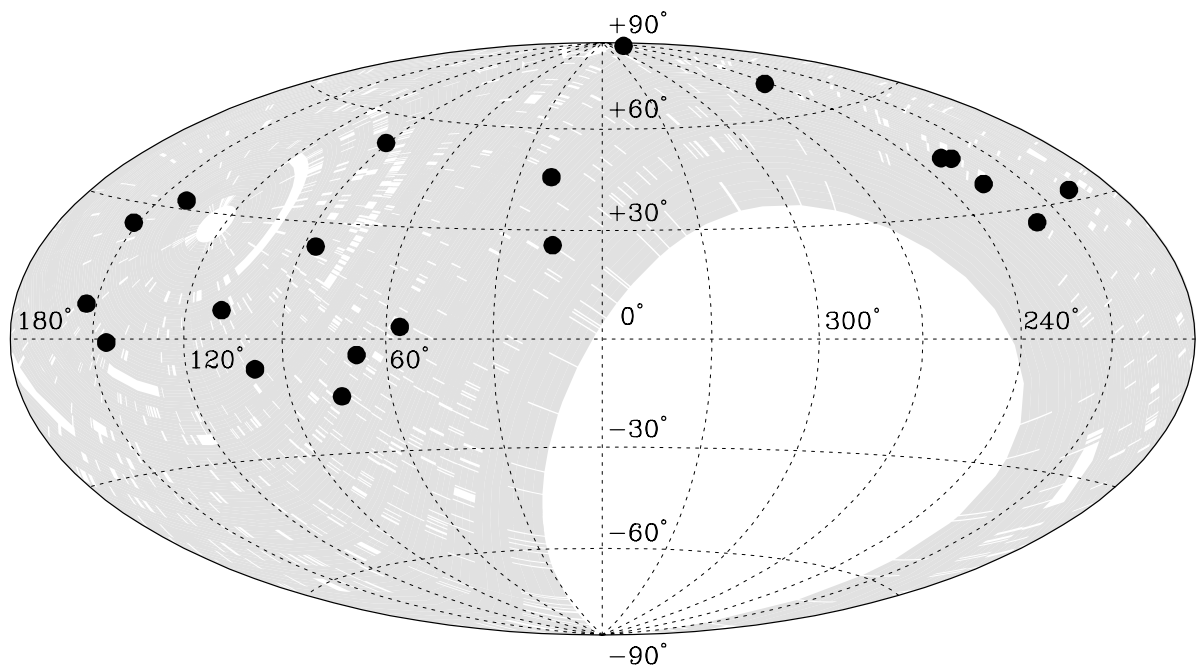


Fig. 2.— Shaded areas indicate sky coverage of the survey in galactic coordinates. Small gaps are the result of local radio interference, and filled circles represent the 20 known pulsars detected in the survey.

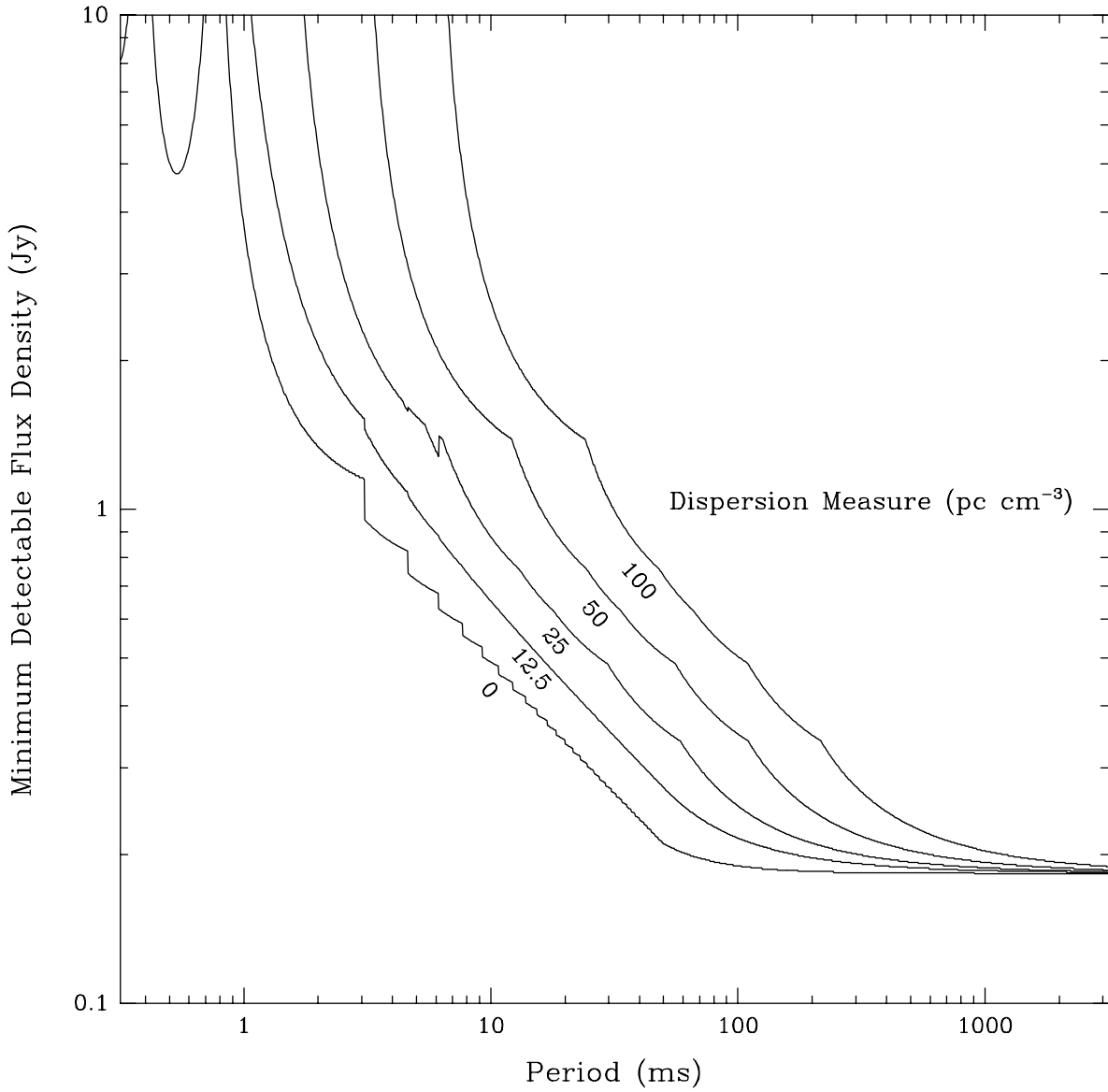


Fig. 3.— Minimum detectable flux density for low duty-cycle pulsars, plotted as a function of period for dispersion measures 0, 12.5, 25, 50, and $100 \text{ cm}^{-3}\text{pc}$. At the higher dispersions, interstellar scattering will degrade sensitivities further.

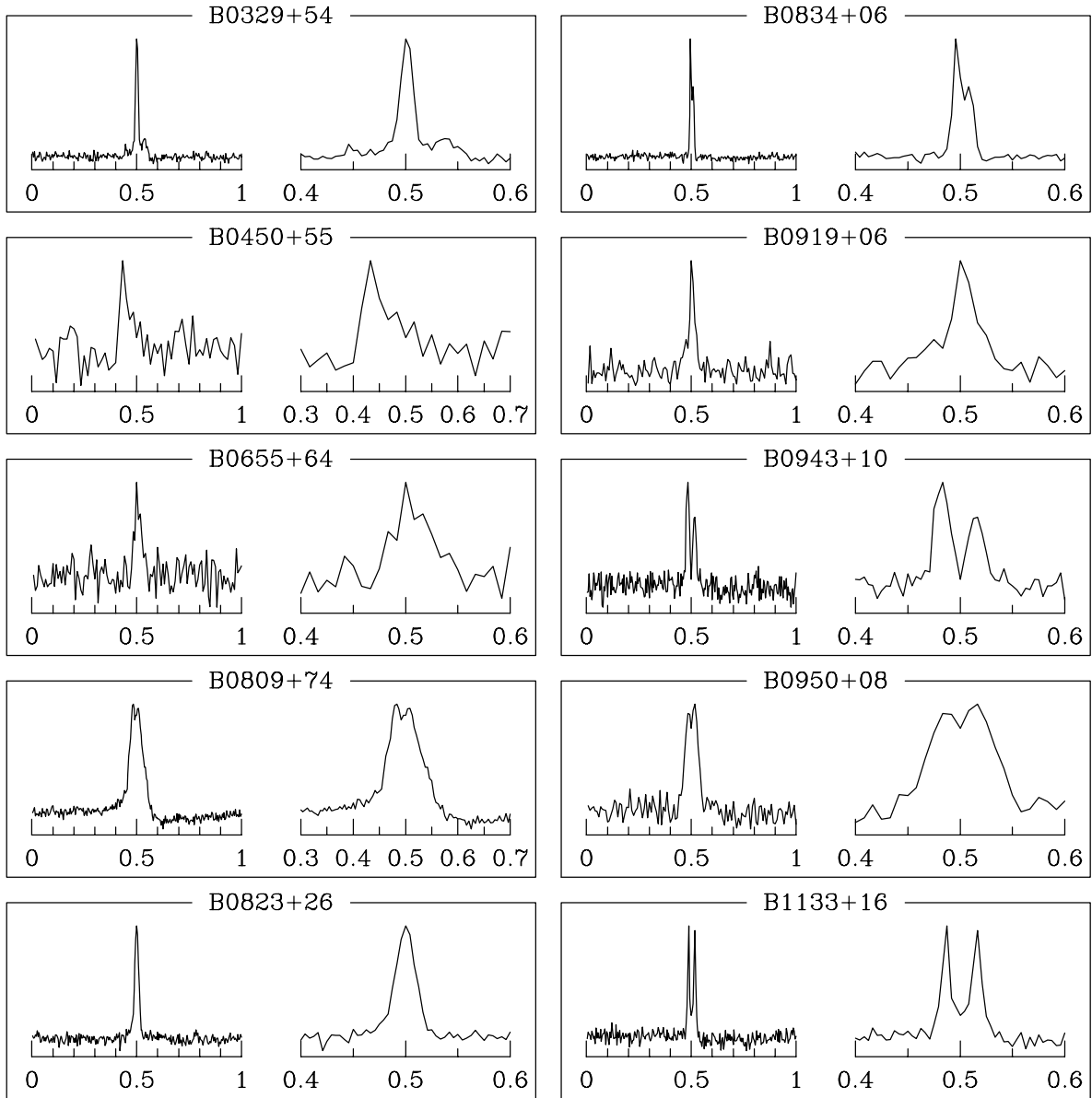


Fig. 4.— Pulse profiles for the 20 detected pulsars, each from a single transit through the telescope beam. Intensity is shown over the entire period (left) and over a smaller region centered on the pulse.

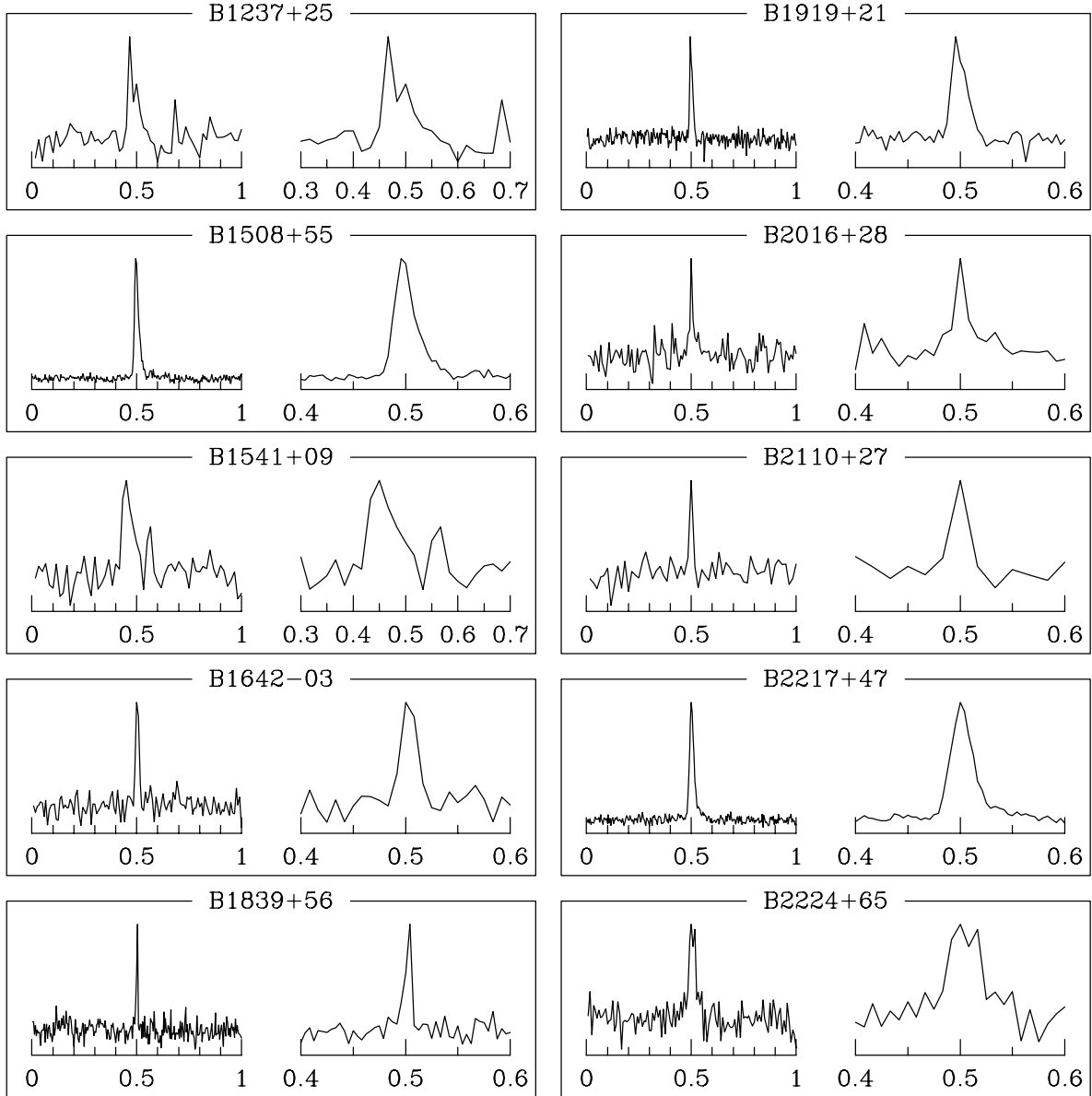


Fig. 4.— Pulse profiles, continued.

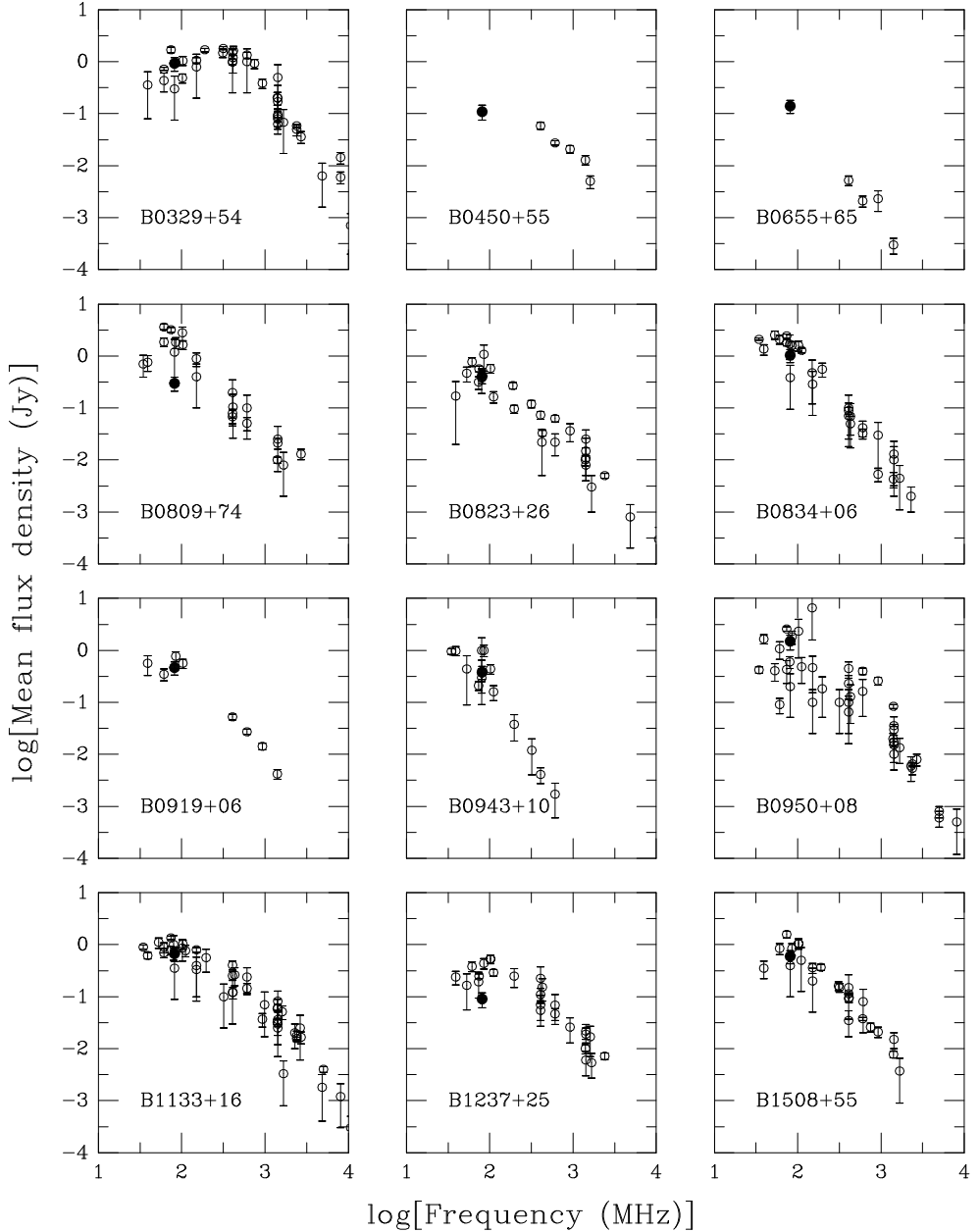


Fig. 5.— Radio frequency spectra of the 20 detected pulsars. Flux density measurements obtained in this survey are plotted as filled circles; those from other studies as open circles. Published results are taken from Slee & Hill 1971, Lyne & Rickett 1968, Pilkington *et al.* 1968, Lorimer *et al.* 1995, Sieber 1973, Izvekova *et al.* 1981, Gupta, Rickett, & Coles 1993, Deshpande & Radhakrishnan 1992, Sieber & Wielebinski 1987, Kuzmin *et al.* 1978, Stinebring & Condon 1990, McLean 1973, Taylor *et al.* 1995.

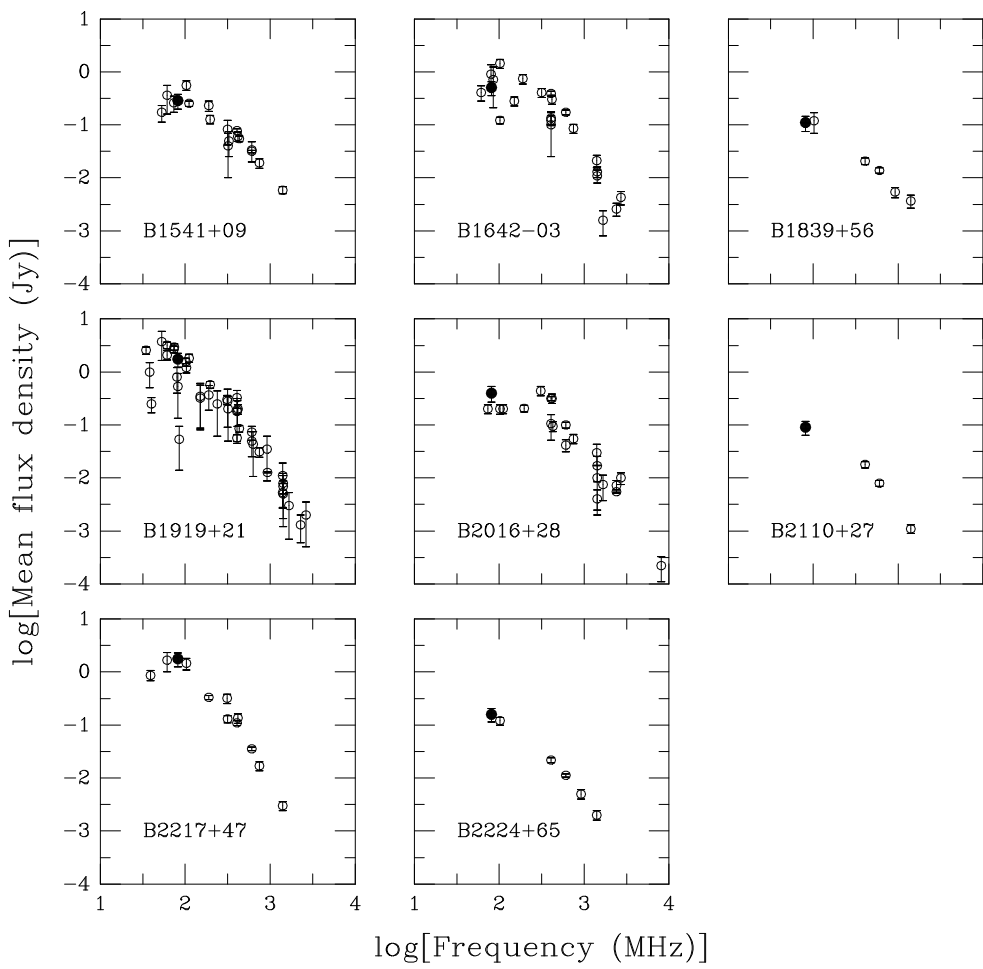


Fig. 5.— Radio frequency spectra, continued.

Table 1: Known pulsars detected in the second Cambridge survey.*

PSR	R. A. (B1950)	Dec. (B1950)	P (s)	DM (cm^{-3}pc)	$\Delta\delta$	\mathcal{R}	S_{400} (mJy)	S_{81} (mJy)
B0329+54	03 ^h 29 ^m 11 ^s	+54°25'	0.715	26.7	0.4°	32.1	35.5	1500
B0450+55	04 50 00	+55 39	0.341	14.6	0.1	<8.5	8.7	59
B0655+64	06 55 49	+64 22	0.196	8.8	1.1	9.5	14.0	5
B0809+74	08 09 03	+74 38	1.192	5.7	0.3	41.5	33.9	79
B0823+26	08 23 51	+26 47	0.531	19.4	0.1	39.9	24.6	73
B0834+06	08 34 26	+06 21	1.274	12.8	0.2	44.3	38.4	89
B0919+06	09 19 35	+06 51	0.431	27.3	0.7	18.0	15.1	52
B0943+10	09 43 27	+10 06	1.098	15.3	0.0	20.8	17.0	4
B0950+08	09 50 31	+08 10	0.253	3.0	1.9	<8.5	13.8	400
B1133+16	11 33 27	+16 08	1.188	4.8	1.0	21.5	22.1	257
B1237+25	12 37 12	+25 10	1.382	9.3	0.2	<8.5	8.9	110
B1508+55	15 08 03	+55 43	0.740	19.5	0.6	43.9	49.4	114
B1541+09	15 41 14	+09 39	0.748	34.9	0.1	<8.5	9.1	78
B1642-03	16 42 25	-03 13	0.388	35.7	0.2	12.5	12.8	393
B1839+56	18 39 51	+56 38	1.653	26.5	1.0	9.7	<8.5	21
B1919+21	19 19 36	+21 47	1.337	12.4	1.6	22.3	24.6	57
B2016+28	20 16 00	+28 31	0.558	14.1	0.9	9.7	<8.5	314
B2110+27	21 10 54	+27 42	1.203	24.7	0.2	<8.5	8.5	18
B2217+47	22 17 46	+47 40	0.539	43.5	1.2	37.4	35.1	111
B2224+65	22 24 17	+65 20	0.683	36.2	0.5	10.5	13.2	22
								1760

*Parameters in the first five columns and S_{400} are from the catalog of Taylor *et al.* (1995; see also Taylor *et al.* 1993).